Article

Label-Free QCM-D monitoring of resveratrol effect on mechanical changes and folate receptor expression levels of living MCF-7 cells: a model for screening of drugs

Shaolian Zhang, Haihua Bai, Jiang Pi, Peihui Yang, and Jiye Cai

Anal. Chem., **Just Accepted Manuscript** • Publication Date (Web): 08 Apr 2015

Label-Free QCM-D monitoring of resveratrol effect on mechanical changes and folate receptor expression levels of living MCF-7 cells: a model for screening of drugs

Shaolian Zhang[1], Haihua Bai[1], Jiang Pi[1], Peihui Yang[1,*], Jiye Cai[1]

1. Department of Chemistry, Jinan University, Guangzhou 510632, People's Republic of China

*Corresponding author:

Peihui Yang, Ph.D, Professor

Department of Chemistry, Jinan University

Guangzhou 510632, China

E-mail address: typh@jnu.edu.cn

Tel/Fax: +86-20-85220223

Shaolian Zhang: zhangshaolian1990@163.com

Abstract

Quartz crystal microbalance with dissipation monitoring (QCM-D) was used for real-time and label-free detection of changes and folate receptor (FR) expression levels on living MCF-7 cells for evaluating the anticancer activity of resveratrol. Here, the mechanical changes of cellular responses to resveratrol was tracked by poly(L-lysine) (PLL) modified QCM-D sensor, and the inhibition effect of resveratrol on FR expression levels on MCF-7 cells was monitored by chitosan-folic acid (CS-FA) composite membrane functionalized Au substrate for the first time. Changes in morphology and cellular state of MCF-7 cell stimulated by resveratrol at different concentrations were detected by inverted fluorescence microscope and flow cytometry. Atomic force microscopy confirmed that resveratrol influenced the cellular mechanical properties. The results indicated that the MCF-7 cells lose its original elasticity and increase its stiffness induced by resveratrol. Confocal fluorescence imaging further observed that resveratrol reduced the FR expression levels on the living cells surface. This study established a typical model of QCM-D biosensor to evaluate the protein biomarker expression levels on cells surface. QCM-D, which was used to investigate potential targets for anti-tumor drug on living cells and realize a better understanding of drug action mechanism, was expected to be developed into a promising tool for screening of drugs.

Keywords: QCM-D; mechanical properties; folate receptor; resveratrol; breast cancer cell

Introduction

Breast cancer cells possess numerous intrinsic properties of cells such as growth, repair, degradation self-diagnosis, and protein and gene expression.[1] They respond in very specific ways to different types of perturbations, allowing them to be used as biointerfaces for the detection of molecules interfering with a cell's activity.[2,3] The cancer cells respond to anticancer agents by complex pathways which often result in altered cell biophysical properties as well as changed expression levels of various cell adhesion molecules and transmembrane protein receptor such as epidermal growth factor receptor.[4,5] Since the above behaviours are significant for evaluating anti-tumor activity of a potential anti-cancer therapeutic agent, a detection system is strongly needed for tracking cellular responses induced by anti-cancer drug.

Traditionally methods, such as flow cytometry, electrochemical biosensor and immunofluorescence assay have been applied to quantitation of the concentration of proteins or other molecules that are involved in the signaling process.[6-11] Although these measurement techniques are generally sensitive and effective, such end-point detection is often limited in providing the actual kinetic information concerning the process of cell signaling. When cellular molecules are tagged with fluorescent labels, their physical activities can be tracked in real time to render kinetic information on cell signaling pathways. However, the presence of fluorescent labels can potentially create a non-native and physiologically irrelevant cellular environment for the molecules of interest,[5,12] which may lead to ambiguous results. A new nanotechnology of atomic force microscopy is shown to be a powerful tool for imaging membrane proteins and measuring the changes in the biophysical properties of the cell.[13,14] Unfortunately, it failed to provide the real-time mechanical properties such as viscoelasticity information. Therefore, a novel assay to investigate membrane proteins and mechanical properties that avoids labor-intensive labeling steps and allows real-time, on-line analysis is worth developing and still the forefront of the field.

Quartz crystal microbalance with dissipation monitoring (QCM-D) is an

ultrasensitive technique, consisting of a piezoelectric quartz crystal in the shape of a thin disk that is made to be part of an electrical circuit.[15,16] The advent of QCM-D has opened new opportunities for assay in flow, yet it is still a challenge and there is large potential for further study.[17] Therefore, it could provide a label-free and real-time measurement of changes in frequency, Δf, and energy dissipation, ΔD, of a layer attached to the quartz surface.[18] Changes in frequency are indicative of changes in mass, while changes in dissipation are indicative of changes in the viscoelastic character of the layer. Since the QCM-D sensor could be able to measures changes in resonance frequency and energy dissipation when a layer of biomolecules adhere to the sensor surface [2], QCM-D and other versions of QCM have been successfully used in various biological analyses.[19] They have become particularly attractive to the field of cell biology because of the capability to monitor cell-surface interactions in a dynamic, label-free, and noninvasive way.[20,21] More recently, even the cell surfaces have been modeled for their protein binding and other characteristics using a similar approach which has also been detailed in some good reviews[22]. Under these scenarios, QCM-D can innovatively and quantitatively determine these cellular events.[23,24] In addition, QCM-D has been applied to measure the changes in the biophysical properties of the cell, such as stiffness, elasticity, adhesion.[2,17,25] Equally important, the interaction between ligand/antibody and its target molecule can also be investigated.[26-28] To our knowledge, however, few QCM-based techniques have been applied to investigate the effect of drug on folate receptor (FR) expression levels on MCF-7 cells. FR, a cell surface receptor, was highly expressed in tumor cells like uterus, breast, brain, lung, kidney cancer cells, while low expression of FR was found in normal tissues.[29] Resveratrol, one kind of antineoplastic agent, shows promising potential in the treatment of different types of cancer cell, such as breast, hepatocellular, gastric and colon.[30,31] Since the anti-tumor signaling pathways are complex, the mechanism of the anti-tumor effects of resveratrol is incompletely understood. As reported, resveratrol can induce tumor cell apoptosis by preventing intracellular regulatory pathways, inhibiting the activity of FR and reducing FR expression levels.[32,33] Therefore, determining FR expression

levels as a target for screening developments of anti-cancer therapeutic agents is worthy for further study.

This report first describes a novel model, a real-time and label-free QCM-D biosensor, for the assessment of the mechanical changes and folate receptor expression levels on MCF-7 cell surface during apoptosis induced by resveratrol. In previous work, a recyclable QCM biosensor was developed using chitosan (CS) and folic acid (FA), generating conjugates that are selectively recognized by MCF-7 cancer cell over-expressed folic acid receptors.[34] Herein, the inhibition effect of resveratrol on the expression of FR on MCF-7 cells was further monitored by the CS-FA composite membrane functionalized QCM-D biosensor. Meanwhile, because cytoskeleton reorganization also alters the mechanical properties such as the viscoelastic character of the resveratrol treated cell [3], poly(L-lysine) (PLL) was used to modify the QCM-D sensor for detecting the energy dissipation.[2] Changes in morphology of cell induced by resveratrol were observed using atomic force microscopy and inverted fluorescence microscope. The cell viability was detected by CCK-8 assay and flow cytometry. Confocal fluorescence imaging further confirmed that resveratrol inhibited FR expression on the MCF-7 cell surface. QCM-D provides the interesting and important view into the drug-induced apoptosis monitoring in real time without any labels. We expect that this method will be useful for screening anti-cancer therapeutic agents and investigating potential targets for drugs.

Experimental

Materials and reagent

Human breast cancer cell lines MCF-7 were donated by Institute of Physiology, Jinan University. RPMI 1640 medium and fetal bovine serum (FBS) were purchased from Gibco Co. Resveratrol (≥98% purity) was purchased from Langze pharmaceutical technology co., LTD. (Nanjing, China). Chitosan (CS, deacetylation degree of 85% and molecular weight of 37.6 KDa) was purchased from Golden-shell Biochemical Co., Ltd. Poly-L-lysine hydrobromide (PLL, Mw ≥ 300,000) was

obtained from Sigma. Nilotinib was a product of Nanjing Ange Pharmaceutical Co. Ltd. (China). Folic acid (FA) was purchased from PEPROTECH Company. Rabbit anti- folate receptor alpha/rhodamin B isothiocyanate (anti-FR alpha/RBITC) was purchased from Beijing biosynthesis Biotechnology Co., LTD. 1-(3-dimethylaminopropyl)-3-ethylcarbodiimide hydrochloride (EDC), N-hydroxysuccinimide (NHS), Phosphate-buffered saline (PBS) solution consisting of 136.7 mmol/L NaCl, 2.7 mmol/L KCl, 9.7 mmol/L Na_2HPO_4 and 1.5 mmol/L KH_2PO_4 was used. All other reagents were of analytical grade, and Millipore Milli-Q water (18 MΩ) was used throughout.

Cell culture

Human breast cancer cell lines MCF-7 were grown in RPMI 1640 culture media supplemented with 100 U/mL streptomycin, 100 U/mL penicillin and 10% fetal bovine serum at 37 ℃ in a humidified atmosphere of 5% CO2. The cells were usually harvested at 95% confluency.

Cell viability assay

The effects of resveratrol on the viability of the aforementioned cells were determined using CCK-8 assay as previously reported.[35] Briefly, 1000 cells per well were plated in triplicate in 96-well plates. After overnight incubation, the cells were treated with varying concentrations of resveratrol (0, 5, 10, 20, 40, 50, 100 μg/mL) for 24 h. The absorbance was then recorded at 450 nm using a microplate reader (SPECTRAmax PLUS384, Molecular Devices, Sunnyvale, USA), and percentage of independent basal levels was calculated.

Morphological imaging

Morphological changes and survival of cells were monitored by obtaining photomicrographs under an inverted phase contrast microscope (Olympus America Inc., Melville, NY) with a digital camera. The nanostructure and Young's modulus of cells were characterized by atomic force microscopy (AFM). The AFM system was

BioScope Catalyst (Bruker, German). The AFM probes were Tap 150Al-G Silicon probes, which purchased from BudgetSensors Company (Bulgaria).

AFM is usually combined with optical microscopy to help select the desired cells. MCF-7 cells were imaged with Tap 150Al-G Silicon AFM probes in ScanAsyst mode, which is an imaging mode with automatic image optimization technology. The material properties and dimensions of the AFM tips used in this experiment were as follows: resonance frequency of 150 kHz (775 kHz), force constant of 5 N/m (72 N/m), cantilever length of 125 μm (710 μm), cantilever width of 25 μm (75 μm), cantilever thickness of 2.1 μm (71 μm), tip radius of 10 nm (72 nm) and tip height of 17 μm (72 μm). For the imaging of living MCF-7 cells in control group, monolayer of cells that firmly attached to the substrate or those that have a flat-shaped morphology were selected to observe in medium solution. In the resveratrol-treated groups, the cells which were not strongly attached to the substrate after resveratrol treatment were fixed by 4% paraformaldehyde at room temperature for 10 min and imaged in air at 256 × 256 pixels resolution and 0.9 Hz scan speed. The scan area was from 30 × 30 μm^2 to 50 × 50 μm^2 depending on the size of the cancer cell. Each set of measurement was performed on five different cells.

Cell apoptosis assay

Cells were harvested as described above and suspended in Hank's Balanced Salt Solution (HBSS). Resveratrol induced apoptosis in MCF-7 cells was determined by flow cytometry using the Annexin V-FITC Apoptosis Detection Kit following the manufacturer's instructions. Briefly, MCF-7 cells were treated with resveratrol (0, 5, 20, 40 μg/mL) for 24 h. The cells were then harvested, washed in PBS and suspended in the binding buffer at 3×10^5 cells/mL. 5 μL of Annexin V-FITC solution and 10 μL of propidium iodide (PI) solution were added to 100 μL of cell suspension. Cells were incubated for 15 min on ice in the dark, and then diluted by adding 400 μL of binding solution. There were no differences in the number of healthy or dead cells as measured using Annexin V/PI staining in cells incubated with resveratrol for up to 2 days (data not shown). All analyses were performed on a flow cytometer (BD

FACSCalibur) equipped with Cell Quest Pro software (BD Bioscience).

Quartz-Crystal Microbalance with Dissipation measurements

A quartz crystal microbalance with dissipation monitoring (KSV QCM-Z500, Q-Sense) was used to record changes in energy dissipation factor (ΔD) and resonant frequency ($\Delta f_n/n$) as a function of time at the order of overtone, n=3. For simplicity, Δf is used to represent $\Delta f_3/3$. The sensing elements used were AT-cut quartz crystals in the form of 14mm-disks with a top surface-coating of a 100 nm thick film of either deposited gold (QSX 301). An electrode was deposited on the bottom surface of each crystal to make it part of an electrical circuit. The frequency and dissipation changes were monitored by instruments of QCM-D, data analysis was performed using QcmZBrwse software from Q-Sense

All binding process was monitored on-line by using a KSV QCM-Z500 instrument at 25 °C with a flow rate of 200 μL/min. Prior to modification, crystal chips (5 MHz) were immersed in a boiling solution (30% H_2O_2, 28% ammonia, and deionized water in a volume ratio of 1: 1: 5 for 5 min. The washed chips were then rinsed thoroughly with deionized water, dried by nitrogen gas prior to use.

For the viscoelasticity assay of the cancer cells, the modified electrode was prepared according to a published procedure.[2] Simply, the cleaned QCM gold electrodes were dipped in 5 mM 3-mercaptopropionic acid (3-MPA) overnight. 3-MPA-modified sensors were rinsed in ethanol and pure water thoroughly and incubated with 1.0 μg/mL of PLL aqueous solution for 12 h, and then rinsed with water thoroughly to remove the weakly adsorbed PLL molecules. After that, the PLL-modified quartz crystal was mounted in a flow module (Q-sense), and the assay buffer at 37 °C was injected. Once the assay buffer was exited through the outlet of the flow module, the flow stopped and the changes in frequency (Δf) and dissipation (ΔD) were recorded simultaneously. After obtaining the stable baselines, flow was resumed by changing the tube to 3×10^5 cells/mL MCF-7 cell solution. The MCF-7 cell sample was injected into the QCM chamber for direct analysis, followed by rinsing with PBS buffer solution to remove non-bound cells. At the end of each

experiment, we count the number of cells on the gold surface. This is to assure that the results correspond to an equivalent amount of cells subject to the experimental condition. In addition, the conjugate of CS-FA prepared in our previous work [34] was spin-coated to the cleaned QCM gold electrode, dried in a silica gel desiccator, and then the quartz crystal was fixed to the QCM chamber. The recognition procedures of MCF-7 cell were similar to the viscoelasticity assay mentioned above. Control experiments for all resveratrol levels carried out on QCM-D modified with only chitosan were also performed. Figure 4A and Figure 5A shows the schematic diagram of preparation of the QCM-D cytosensor.

Confocal fluorescence imaging of FR on MCF-7 cells

The fluorescence labeling procedures for rabbit anti-FR alpha/RBITC and DAPI were as follows: MCF-7 cells treated with different concentrations of resveratrol for 24 h were washed three times with PBS buffer. After that, cells were fixed by 2.5% glutaraldehyde for 15 min and washed three times by PBS buffer prior to staining. 1% bovine serum albumin was used to block the cells for 15 min. Then, cells were incubated with 200 μL rabbit anti-FR alpha/RBITC (200 nM) at 37°C for 30 min and 100 μL DAPI (0.1μg/mL) for 4 min. Then cells were washed thrice with buffer and imaged by a Carl Zeiss LCM 510 Meta Duo Scan laser scanning confocal microscope. The images were processed by Zeiss LSCM-equipped software.

Results and discussion

Effect of resveratrol on cell viability by the CCK-8 assay

CCK-8 assay was performed to quantitatively evaluate cytotoxicity of resveratrol in human breast cancer cell line MCF-7. CCK-8 is metabolized to a purple formazan salt by mitochondrial enzymes in living cells, and the absorbance is thus proportional to the number of viable cells. It is obvious from Fig. 1A that the cell viability exhibited a dose-dependent markedly inhibited growth on MCF-7. Cell survival rates of the MCF-7 cells, which were 100%, 79%, 55%, 41%, 38% and 5% for control, 5, 10, 20, 40, 50 and 100 μg/mL resveratrol treated with MCF-7 cells, respectively. The

IC_{50} value was 26.32 ± 3.50 μg/mL. In addition, after treated cell with 26.32 μg/mL of resveratrol for 0, 6, 12, 24, 48 h, respectively, cell survival rates of the MCF-7 cells decreased with the increase of the treatment of time, as described in Fig. 1B. The results implied that resveratrol was cytotoxic to MCF-7 cells both in a dose-dependent and in a time-dependent manner significantly.

Effect of resveratrol on cell morphology

Further, the inverted fluorescence microscope and atomic force microscopy were used to visualize the growing status and the morphology of MCF-7 cell treated with resveratrol. As shown in Fig. S1, the growing status of MCF-7 cells treated with different concentration of resveratrol was observed by inverted fluorescence microscope. Cells treated without resveratrol grew in a higher density with typically of long-spindle shape. Obviously, after being treated with high concentration of resveratrol, the MCF-7 cells growth was inhibited and showed apoptosis. Meanwhile, Fig. 2 shows the three dimensional images of single MCF-7 cell treated with 0, 40, 100 μg/mL resveratrol for 24 h. In the control group, the cell membrane was relatively smooth and intact. Cell revealed typical long-spindle shaped morphology and obvious pseudopodium. With the increasing treatment concentration of resveratrol, obvious morphology changes were observed, such as shrinkage and roundout, even collapse. Pseudopodium disappeared and the cell membranes were damaged.

Flow cytometry assay cell apoptosis

To further assess the apoptotic cells induced by resveratrol, flow cytometric (FCM) analysis of the MCF-7 cells labeled with FITC-Annexin V was performed. As shown in Fig. 3, with treatment of resveratrol for 24 h, the percentage of the population of PI (-) and Annexin V (+) cells, corresponding to early apoptosis, was increased as the addition of resveratrol concentration. The percentage of living cells is 92.7% for non-treatment as described in Fig. 3A. When the incubation with 5 μg/mL resveratrol lightly decreased the number of MCF-7 living cells (Fig. 3B). Furthermore, after being treated with 20 μg/mL resveratrol, the early apoptosis rate shown 21.0% in

Fig. 3C. Obviously, when the resveratrol was 40 μg/mL, the early apoptosis was at highest rate 56.7% for treatment group (Fig. 3D). These results demonstrated that resveratrol could induce MCF-7 cells apoptosis, which closely matched to those obtained from the above microscopic observations.

Characterized the mechanical properties of the resveratrol treated MCF-7 cells by QCM-D

Cell mechanical properties especially cell membrane viscoelasticity and stiffness have been identified as important factors relating to cell function, adherence, motility, transformation, and invasion.[25] The energy dissipation (ΔD) and resistance change (ΔR) acquired by QCM-D can give a qualitative measure of how viscoelasticity and rigidly the cell adheres to the underlying substrate as reported previously.[36] Herein, poly(L-lysine) (PLL) was used as a substrate material to enhance cell adhesion to the surface of Au chip via in vitro cell cultivation based on its good biocompatibility, plentiful active amino groups, flexible molecular backbone, and relatively good solubility in water.[37] Fig. 4A shows the preparation of QCM-D cytosensor.

As shown in Fig. 4B, the short-term, MCF-7 cell viscoelasticity responses to resveratrol were monitored by QCM-D, ΔD and ΔR shifts reflect time-dependent changes in mechanotransduction and mechanical properties of the basal region of the MCF-7 cells treated with 0, 20, 40, 60, 80, 100 μg/mL resveratrol for 24 h. As shown in the data plot (Fig. $4B_1$), stable baselines were achieved for all experiments prior to the addition of treated cells. In the control group, the change in dissipation was around 1.8×10^{-4} (RSD=4.3%, n=3), which means the cells possess its intrinsic viscoelasticity. Interesting, with the increasing treatment concentration of resveratrol, obvious negative changes in dissipation were observed, indicating that cells were damaged by resveratrol, and thus lose its original elasticity, which would lead to the increasing stiffness of cell. Compared to curve e in figure $4B_1$, after being treated with 100 μg/mL resveratrol (curve f), the viscoelasticity of cells had no significant changes due to cell apoptosis. Meanwhile, slightly changes in dissipation with the increasing treatment of concentration of resveratrol were obtained. This is due to the drug

weakened cell activity and thus limited the capacity of reconstructing cytoskeleton. The same results can be seen in Fig. $4B_2$, and ΔR also indicating the rigidly change of resveratrol treated cell. In a word, induced by drug, the cytoskeleton, membrane proteins and surface electric charge on cell membrane had been influenced, thus changed the viscoelasticity and rigidity of the cell, than decreased the adhesion to the surface of PLL modified biosensor and lead to the signals of decreased ΔD and increased ΔR.

To further study the effect of resveratrol on viscoelasticity of MCF-7 cell, the cells were treated with 26.32 μg/mL (IC_{50}) resveratrol for different periods of time. Fig. $4C_1$ shows the time course of the energy dissipation when the treated MCF-7 cells were injected in chamber. It was obviously observed that the MCF-7 cells reveal good viscoelasticity in the control group. However, negative changes in dissipation were obtained as the longer time treated to cells, which can be due to the cell damaged by resveratrol as time goes by. It indicated the relationship between the cytotoxicity of resveratrol and the biomechanical properties of the cells. The visualized change of energy dissipation can be seen in the inset of Fig. $4C_1$, apoptosis occurred for almost treated cells to about 24 h, and turned completely rigid. In addition, the dissipation signal would not be returned completely to the initial baseline, which is due to proteins or adhesion molecules from apoptosis of MCF-7 cells would flow in the gap between detached cell and substrate.

Young's modulus measured by atomic force microscopy further confirmed the above results. As shown in Fig. $4C_2$, the control group of MCF-7 cells showed an average Young's modulus of 13.05 ± 2.03 kPa, while after treated with 40 μg/mL and 100 μg/mL resveratrol for 24 h, much higher Young's modulus were obtained showed an average Young's modulus of 28.91 ± 3.43 kPa and 168.74 ± 8.93 kPa, respectively. It demonstrated that the positive correlation between the stiffness of cells and drug concentration. As Young's modulus was the evaluation indicator of elasticity, these results indicated that MCF-7 cells were damaged by drug like resveratrol, and appeared to be much stiffer. All these results well confirmed the signal obtained by QCM-D, indicating that the sensitive QCM-D technique has a potential to apply in

bio-analysis.

Detection of the FR expressed on MCF-7 cell surface by QCM-D

In order to investigate whether resveratrol treatment could influence the expression of membrane protein on the MCF-7 cell surface, a sensitive CS-FA functionalized QCM-D biosensor was constructed to recognize folate receptor on the living MCF-7 cells surface, as shown in Fig. 5A. In this way, we aimed to build a model, which could evaluate the anticancer activity of drug based on the specific protein expression levels on cells membrane or biophysical properties of cancer cells.

Fig. 5B shows the real-time capturing of the MCF-7 cell using the CS-FA modified biosensor. After obtained the baseline by injecting PBS buffer, the inflow of MCF-7 cell caused the increase of mass on the Au substrate showing the decrease of frequency (Δf). As shown in Fig. $5B_1$, when the same number of resveratrol treated cells were recognized by the sensor, $-\Delta f$ showed an decrease as the increase of drug concentration. This might be due to resveratrol-treated MCF-7 cells expressed less FR molecules, which resulted in the less of MCF-7 cells binding to the QCM-D biosensor. Nevertheless, when the cells were treated with 100 μg/mL resveratrol, the frequency response was significantly reduced to about 20 Hz. The influencing factors of the frequency changes could be that cell apoptosis and the apoptosis body detaching from the CS-FA modified Au substrate and then caused the decrease of mass on the Au surface. Simultaneously, just like the dissipation signal, the frequency value would not be returned completely to the initial baseline for some protein or adhesion molecules from cells attaching the substrate. In addition, a good linear range may exist in Fig. $5B_2$ over the concentration of resveratrol, which will be focused in the further study. For comparison, the results of control experiments for all resveratrol levels carried out on QCM-D modified with only chitosan were shown in Fig. $5B_2$. Obviously, the Δf values were too small due to the negligible non- nonspecific binding of cells. Thus, as a model, this proposed CS-FA based QCM-D biosensor could be successful to detect the FR expressed on MCF-7 cell surface.

Furthermore, the frequency response of MCF-7 cells after exposured to 26.32

μg/mL (IC_{50}) resveratrol for 0, 6, 12, 24 and 48 h were tracked by QCM-D. As shown in Fig. $5C_1$, the changes of frequency obtained show significant dependence on the resveratrol treatment time. Δ*f* of cells in control group are maximum due to FR highly expressed in tumor, as expected by the frequency changes of dose-dependent shown in Fig. $5B_1$ (curve a). In the treated cells, the values of Δ*f* decreased with the time of drug treatment, indicating a time-dependent. The presentation of the Δ*f* histograms obtained by measuring five times on treated cells were shown in the inset of Fig. $5C_1$. It was obvious that the Δ*f* had dramatically decreased to 120 Hz due to less expression of FR on cells surface after treated for 24 h, leading to a less of MCF-7 captured by the CS-FA based QCM-D biosensor. Actually, when the cells were treated with 26.32 μg/mL resveratrol for more than 24 h, almost all the living cells were damaged in varying degrees. Naturally, the apoptotic bodies or proteins would adhesion to the modified Au substrate due to specificity or non-specificity. In this case, the mass on the Au surface would be increase showing the decrease of frequency, and thus the frequency signal would not be returned completely to the initial point.

As a model, the specificity and selectivity of the proposed QCM-D cytosensing strategy is of great importance to appraise its feasibility. As shown in the left of Fig. $5C_2$, 3×10^5 cells/mL MCF-7 cells recognized to the CS modified QCM-D biosensor showed a slight Δ*f* signals(a), while after recognized to the CS-FA modified biosensor, obvious Δ*f* signals occurred due to FA specificity binding to FR over-expressed on MCF-7 cell surface (b). Moreover, when the cells were treated with saturated FA, the average value of Δ*f* was only 120 ±18.6 Hz (c). After the cells were treated with half amount of FA, the Δ*f* increased (d). Since the FA could recognize the residual FR on MCF-7 cell surface, and further, cells could be captured by the CS-FA modified QCM-D biosensor. In addition, the selectivity of the biosensor was shown in the right side of Fig. $5C_2$, the blank and the adsorptions of human vascular endothelial cells (EC), oral epithelial cells (OEC) on CS-FA based biosensor were all negligible. By contrast, the binding of CS-FA with 3×10^5 cells/mL MCF-7 cells resulted in a much larger frequency shift. Moreover, a significant frequency change was observed in the mixture of endothelial cells, oral epithelial cells and MCF-7 cells. The above results

indicated this QCM-D biosensor showing good specificity and selectivity.

Fluorescence imaging of FR distribution on MCF-7 cells surface

The fluorescence labeling technology was used to visualize the expression of FR on cell surface with or without resveratrol treatment. The positions of red and blue fluorescence represented FR and the nuclei, respectively. As shown in Fig. 6A, cells in control group were typically of long-spindle shape and strong fluorescence intensity was observed. After being treated with 5 μg/mL resveratrol, the fluorescence of the cells had no significant changes, while the shape of cells turned round slightly (Fig. 6B). When MCF-7 cells were treated with 10 μg/mL resveratrol, the cell morphology was deformed. The cells were not plump but shrank showed in Fig. 6C. Furthermore, after being treated with 40 μg/mL resveratrol, the shape of MCF-7 cells turned round and the fluorescence intensity was significantly reduced (Fig. 6D). Fig.6 A_2-D_2 also shows that the cell nucleus shrink slightly after being treated with resveratrol. Experimental results indicated that resveratrol reduced the FR expression levels on the living cells surface.

Conclusion

QCM-D provides a novel approach for monitoring the short-term responses of cells to resveratrol induced apoptosis signaling by tracking of changes in the dissipation and frequency responses of cells attached to a surface. Our study revealed that changes in dissipation, ΔD, are associated with the remodeling of the cytoskeleton and represent the cellular viscoelasticity. Changes in frequency, Δf, are associated with the FR expression levels on living MCF-7 cells and indicate the anti-tumor effect of resveratrol. The results, which were also confirmed by flow cytometry and confocal microscopy assay and other biotechnologies, showed that resveratrol influenced the cellular state and reduced expression of FR on MCF-7 cells both in dose-dependent and time-dependent manners. To our knowledge, this is the first example of tracking cell apoptosis signaling based on the measurement of cellular mechanical and FR expression levels on MCF-7 cells. Take the advantage of

this model, we envision that the unique capability of QCM-D to evaluate the potential anti-cancer drug and will complement the existing approach to prognosis of cancer. Moreover, mechanical properties of cells have become the subject of considerable scientific research because of the potential link between these properties and human diseases.[38] With a quantifiable measure of cytoskeleton remodeling based on energy dissipation of cells, QCM-D offers a noninvasive alternative for tracking changes in mechanical properties of the cells in a real-time and continuous manner. This may also help obtain a fundamental understanding of the correlation between cell function and cell mechanical properties.

Acknowledgment

This work was supported by grants from National Natural Science Foundation of China (No. 21375048), the Major State Basic Research Development Program of China (973 Program) (No. 2010CB833603).

References

(1) Cross, S. E.; Jin, Y.-S.; Rao, J.; Gimzewski, J. K. *Nature Nanotechnology* **2007**, *2*, 780-783.

(2) Bhirde, A. A.; Chikkaveeraiah, B. V.; Srivatsan, A.; Niu, G.; Jin, A. J.; Kapoor, A.; Wang, Z.; Patel, S.; Patel, V.; Gorbach, A. M.; Leapman, R. D.; Gutkind, J. S.; Walker, A. R. H.; Chen, X. *Acs Nano* **2014**, *8*, 4177-4189.

(3) Fatisson, J.; Azari, F.; Tufenkji, N. *Biosensors and Bioelectronics* **2011**, *26*, 3207-3212.

(4) Tan, L.; Lin, P.; Pezeshkian, B.; Rehman, A.; Madlambayan, G.; Zeng, X. *Biosensors and Bioelectronics* **2014**, *56*, 151-158.

(5) Chen, J. Y.; Li, M.; Penn, L. S.; Xi, J. *Analytical Chemistry* **2011**, *83*, 3141-3146.

(6) Thariat, J.; Etienne-Grimaldi, M.-C.; Grall, D.; Bensadoun, R.-J.; Cayre, A.; Penault-Llorca, F.; Veracini, L.; Francoual, M.; Formento, J.-L.; Dassonville, O.; De Raucourt, D.; Geoffrois, L.; Giraud, P.; Racadot, S.; Moriniere, S.; Milano, G.; Van Obberghen-Schilling, E. *Clinical Cancer Research* **2012**, *18*, 1313-1322.

(7) Bloemberg, D.; Quadrilatero, J. *Biochimica et Biophysica Acta (BBA) - Molecular Cell Research* **2014**, *1843*, 2926-2936.

(8) Ishii, J.; Oda, A.; Togawa, S.; Fukao, A.; Fujiwara, T.; Ogino, C.; Kondo, A. *Analytical Biochemistry* **2014**, *446*, 37-43.

(9) Akter, R.; Rahman, M. A.; Rhee, C. K. *Analytical Chemistry* **2012**, *84*, 6407-6415.

(10) Zhang, S.; Zhang, L.; Zhang, X.; Yang, P.; Cai, J. *Analyst* **2014**, *139*, 3629-3635.

(11) Hu, C.; Yang, D.-P.; Wang, Z.; Huang, P.; Wang, X.; Chen, D.; Cui, D.; Yang, M.; Jia, N. *Biosensors and Bioelectronics* **2013**, *41*, 656-662.

(12) Wang, Z.; Zhang, X.; Wang, Y.; Gao, J.; Li, Z. *Acta Chimica Sinica* **2013**, *71*, 1620-1624.

(13) Chopinet, L.; Formosa, C.; Rols, M. P.; Duval, R. E.; Dague, E. *Micron* **2013**, *48*, 26-33.

(14) Canale, C.; Petrelli, A.; Salerno, M.; Diaspro, A.; Dante, S. *Biosensors and Bioelectronics* **2013**, *48*, 172-179.

(15) Yang, L.; Jiang, L.; Yao, W.; Liu, J.; Han, J. *Langmuir* **2014**, *30*, 9962-9971.

(16) Webster, A.; Vollmer, F.; Sato, Y. *Nature Communications* **2014**, *5*.

(17) Song, L.; Sjollema, J.; Sharma, P. K.; Kaper, H. J.; van der Mei, H. C.; Busscher, H. J. *Acs Nano* **2014**, *8*, 8457-8467.

(18) Ehmann, H. M. A.; Mohan, T.; Koshanskaya, M.; Scheicher, S.; Breitwieser, D.; Ribitsch, V.; Stana-Kleinschek, K.; Spirk, S. *Chemical Communications* **2014**, *50*, 13070-13072.

(19) Speight, R. E.; Cooper, M. A. *Journal of Molecular Recognition* **2012**, *25*, 451-473.

(20) Li, X.; Pei, Y.; Zhang, R.; Shuai, Q.; Wang, F.; Aastrup, T.; Pei, Z. *Chemical Communications* **2013**, *49*, 9908-9910.

(21) Peiris, D.; Markiv, A.; Curley, G. P.; Dwek, M. V. *Biosensors & Bioelectronics* **2012**, *35*, 160-166.

(22) Cheng, C. I.; Chang, Y.-P.; Chu, Y.-H. *Chemical Society Reviews* **2012**, *41*, 1947-1971.

(23) Abdelwahab, A. A.; Koh, W. C. A.; Noh, H.-B.; Shim, Y.-B. *Biosensors & Bioelectronics* **2010**, *26*, 1080-1086.

(24) Tarantola, M.; Marel, A.-K.; Sunnick, E.; Adam, H.; Wegener, J.; Janshoff, A. *Integrative Biology* **2010**, *2*, 139-150.

(25) Sarna, M.; Zadlo, A.; Hermanowicz, P.; Madeja, Z.; Burda, K.; Sarna, T. *Experimental dermatology* **2014**, *23*, 813-818.

(26) Gou, Y.; Geng, J.; Richards, S.-J.; Burns, J.; Becer, C. R.; Haddleton, D. M. *Journal of Polymer Science Part a-Polymer Chemistry* **2013**, *51*, 2588-2597.

(27) Hatty, C. R.; Le Brun, A. P.; Lake, V.; Clifton, L. A.; Liu, G. J.; James, M.; Banati, R. B. *Biochimica Et Biophysica Acta-Biomembranes* **2014**, *1838*, 1019-1030.

(28) Chen, J. Y.; Shahid, A.; Garcia, M. P.; Penn, L. S.; Xi, J. *Biosensors & Bioelectronics* **2012**, *38*, 375-381.

(29) Polyák, A.; Hajdu, I.; Bodnár, M.; Dabasi, G.; Jóba, R. P.; Borbély, J.; Balogh, L. *International Journal of Pharmaceutics* **2014**, *474*, 91-94.

(30) Saud, S. M.; Li, W.; Morris, N. L.; Matter, M. S.; Colburn, N. H.; Kim, Y. S.; Young, M. R. *Carcinogenesis* **2014**, *35*, 2778-2786.

(31) Cerella, C.; Teiten, M. H.; Radogna, F.; Dicato, M.; Diederich, M. *Biotechnology Advances* **2014**, *32*, 1111-1122.

(32) Kansara, V.; Paturi, D.; Luo, S.; Gaudana, R.; Mitra, A. K. *International Journal of Pharmaceutics* **2008**, *355*, 210-219.

(33) Couto, M. R.; Goncalves, P.; Catarino, T.; Araujo, J. R.; Correia-Branco, A.; Martel, F. *Cell Biology and Toxicology* **2012**, *28*, 369-381.

(34) Zhang, S.; Bai, H.; Luo, J.; Yang, P.; Cai, J. *The Analyst* **2014**, *139*, 6259-6265.

(35) Ma, Y.; Zhang, J.; Zhang, Q.; Chen, P.; Song, J.; Yu, S.; Liu, H.; Liu, F.; Song, C.; Yang, D.; Liu, J. *Biochemical and Biophysical Research Communications* **2014**, *448*, 8-14.

(36) Marx, K. A.; Zhou, T.; Montrone, A.; McIntosh, D.; Braunhut, S. J. *Analytical Biochemistry* **2005**, *343*, 23-34.

(37) Canale, C.; Petrelli, A.; Salerno, M.; Diaspro, A.; Dante, S. *Biosensors & Bioelectronics* **2013**, *48*, 172-179.

(38) Mierke, C. T. *Reports on Progress in Physics* **2014**, *77*.

Figure captions

Fig. 1 (A) CCK-8 Cell growth inhibition assays of resveratrol. MCF-7 Cells were treated with 0, 5, 10, 20, 40, 50, 100 μg/mL of RVL for 24 h, respectively. (B) The MCF-7 cell viability after treated with 26.32 μg/mL of resveratrol for 0, 6, 12, 24, 48 h, respectively. All data were collected from three measurements and the error bars indicated the standard deviation.

Fig. 2 Representative three dimensional AFM images of MCF-7 cells treated with 0, 40, 100 μg/ml resveratrol for 24 h. The colors in the images indicate different heights with light and dark colors corresponding to higher and lower topography.

Fig. 3 MCF-7 cells were treated with different concentrations of resveratrol for 24 h and harvested for apoptosis assay by flow cytometry using PI and Annexin V-FITC double staining. Resveratrol concentration (A-D): 0, 5, 20, 40 μg/mL.

Fig. 4 QCM-D investigated the viscoelasticity of the resveratrol treated MCF-7 cells. (A) Construction process of QCM-D cytosensor based on PLL membrane. (B) Real-time QCM-D responses. Changes in dissipation (B1) and resistance (B2) values as MCF-7 cells undergo treatment with different concentrations of RVL for 24 h in the quartz crystal microbalance. Concentration of RVL (a-f): 0, 20, 40, 60, 80, 100 μg/mL. (C) QCM-D real-time dissipation response. QCM-D investigated the viscoelasticity (C1) of the MCF-7 cells treated with 26.32 μg/mL (IC_{50}) resveratrol for 0, 6, 12, 24, 48 hours. Inset: column graph illustrated the viscoelasticity changes. (C2) shows histogram of Young's modulus of cells. The error bars represent the standard deviation (S.D.) of five measurements.

Fig. 5 QCM-D investigated the FR expressed on the resveratrol treated MCF-7 cell surface. (A) Construction process of QCM-D cytosensor based on CS-FA membrane.

(B and C) shows the real-time QCM-D frequency responses. (B1) Real-time QCM-D frequency responses to MCF-7 cells undergo treatment with different concentrations of resveratrol for 24 h. The total number of cell recognized by QCM-D biosensor is 3×10^5 in each experiment. Concentration of RVL (a-f): 0, 20, 40, 60, 80, 100 μg/mL. (B2) The fitting relationships between the frequency shifts and resveratrol concentrations were established, green dots represent the frequency signals from CS-FA modified QCM-D biosensor; Pink dots show the frequency signals from QCM-D modified with only chitosan (control experiments). (C1) QCM-D investigated the frequency responses of the MCF-7 cells treated with 26.32 μg/mL (IC_{50}) of resveratrol for 0, 6, 12, 24, 48 hours. Inset: column graph illustrated the frequency changes. (C2) Left shows the Δf signals of MCF-7 cells recognized to the (a) CS and (b-d) CS-FA modified QCM biosensor, (b) without treatment, (c) after treated the cells with saturated FA and (d) half amount of FA; Right shows the selectivity of the CS-FA modified QCM-D biosensor, endothelial cells (EC), oral epithelial cells (OEC), endothelial cells, oral epithelial cells and MCF-7 cells (Mixture); Cell concentration is 3×10^5 cells/mL. The error bars represent the standard deviation (S.D.) of five measurements.

Fig. 6 Confocal fluorescence images of FR distribution on MCF-7 cells treated without resveratrol (A) and with various concentrations (5, 20, 40 μg/mL) of resveratrol (B, C, D) for 24 h. The position of red fluorescence (A1, B1, C1 and D1) represents RBITC-labeled anti-FR anti-FR alpha which binds specifically to FR and blue fluorescence (A2, B2, C2, D2) represents the position of nuclei of MCF-7cells stained with DAPI. The merged images of red fluorescence with blue fluorescence images are shown in A3, B3, C3 and D3, respectively. Scale bar: 20 μm.

Graphic abstract

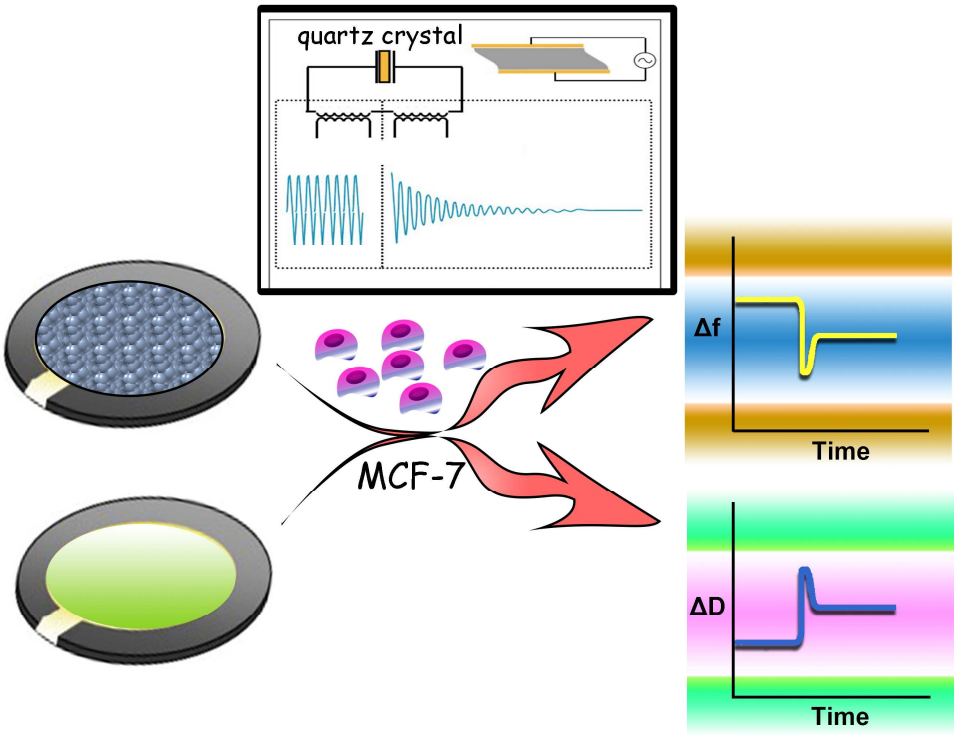

Figures

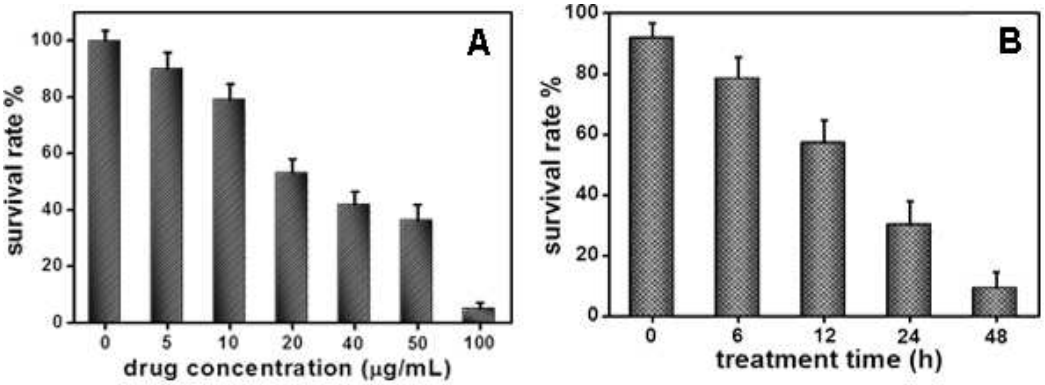

Fig. 1

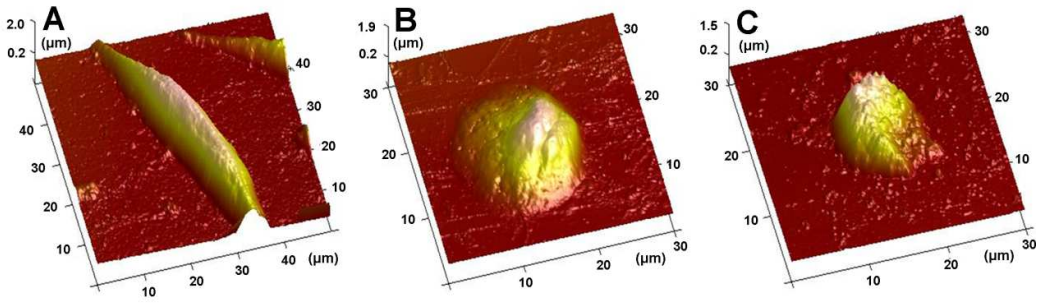
A
B
C
(μm)

Fig. 2

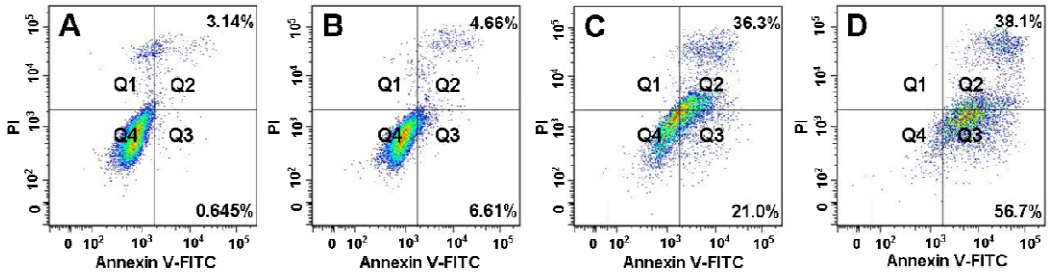
A
3.14%
Q1
Q2
Q4
Q3
0.645%
B
4.66%
6.61%
C
36.3%
21.0%
D
38.1%
56.7%
PI
Annexin V-FITC

Fig. 3

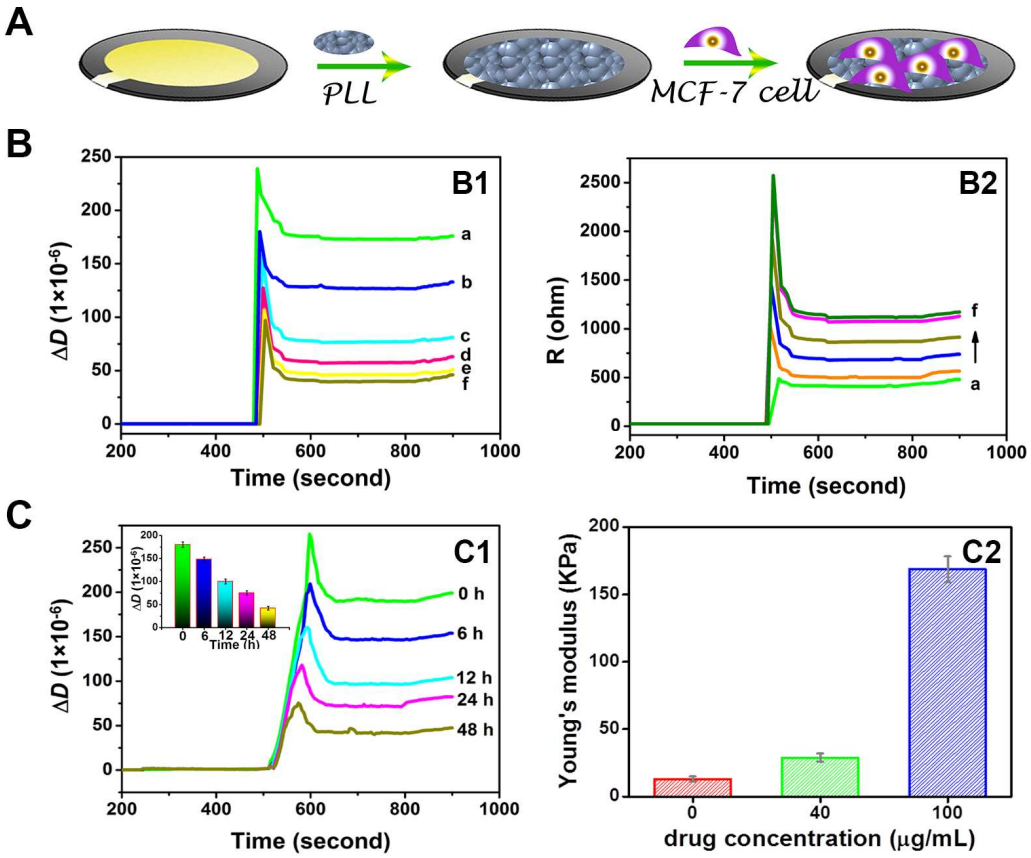
A
PLL
MCF-7 cell
B
B1
ΔD (1×10-6)
Time (second)
a
b
c
d
e
f
B2
R (ohm)
Time (second)
C
C1
ΔD (1×10-6)
Time (second)
0 h
6 h
12 h
24 h
48 h
Time (h)
C2
Young's modulus (KPa)
drug concentration (μg/mL)

Fig. 4

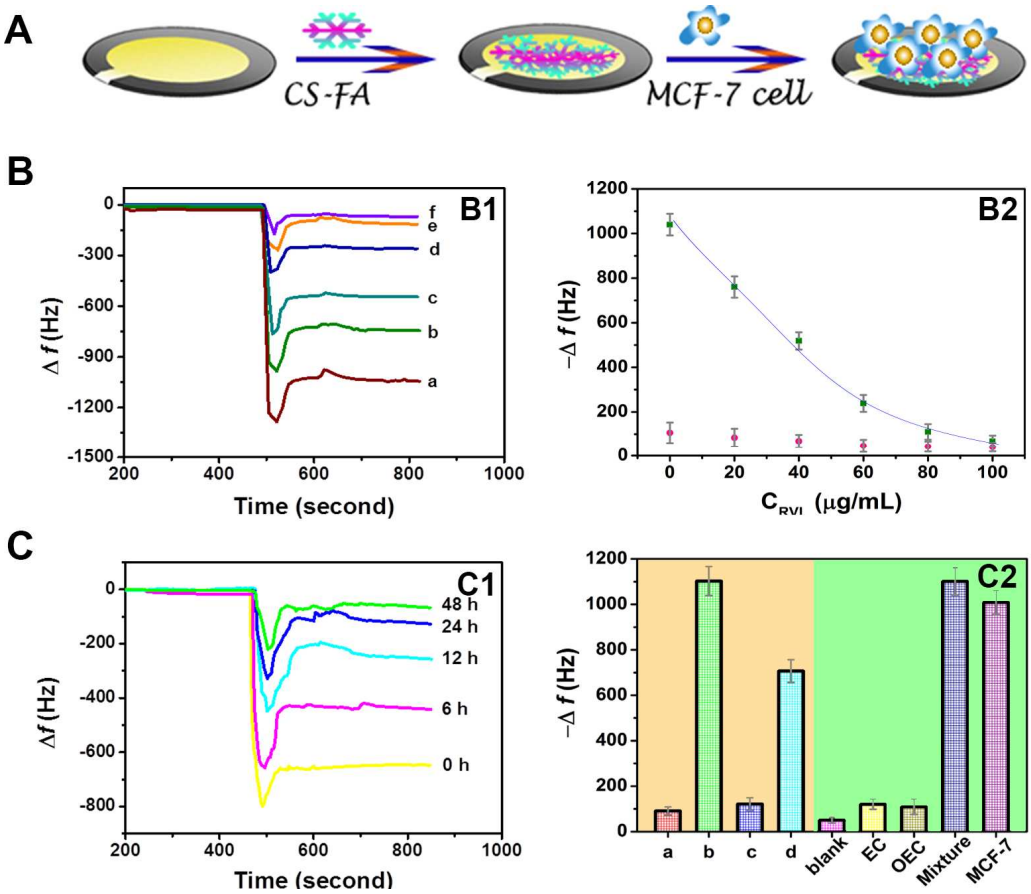
A
CS-FA
MCF-7 cell
B
B1
f
e
d
c
b
a
Δ f (Hz)
Time (second)
B2
−Δ f (Hz)
C_RVI (μg/mL)
C
C1
48 h
24 h
12 h
6 h
0 h
Δf (Hz)
Time (second)
C2
−Δ f (Hz)
a
b
c
d
blank
EC
OEC
Mixture
MCF-7

Fig. 5

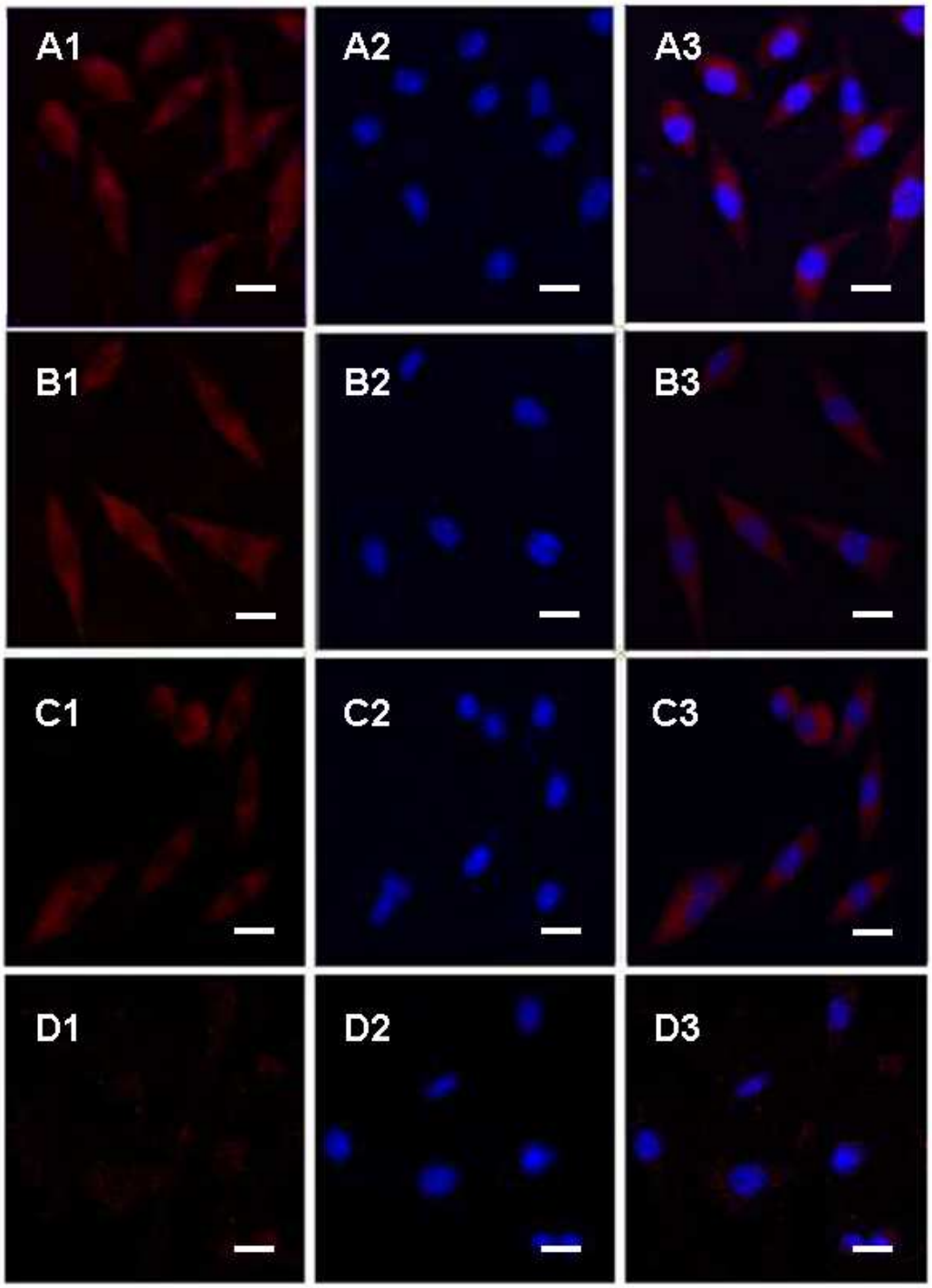

Fig. 6